Spatial Resolution and Imaging of Gamma-Rays with Germanium Strip Detectors

R.A. Kroeger, W.N. Johnson, R.L. Kinzer, J.D. Kurfess
Naval Research Laboratory
Washington, DC 20375

S.E. Inderhees, B. Phlips
Universities Space Research Association
Washington, DC

N. Gehrels
Goddard Space Flight Center
Greenbelt, MD 20771

B. Graham
George Mason University
Fairfax, VA

ABSTRACT

Germanium strip detectors combine high quality spectral resolution with two-dimensional positioning of γ-ray interactions. Readout is accomplished using crossed electrodes on opposite faces of a planar germanium detector. Potential astrophysics applications include focal plane detectors for coded-aperture or grazing incidence X-ray mirror imagers, and as detection elements of a high resolution Compton telescope. We report on test results of two germanium strips detectors, one with 2 mm position resolution, the other with 9 mm. We will discuss general device performance in terms of energy and position resolution, crosstalk effects, potential applications and a demonstration of imaging properties.

Keywords: germanium detectors, strip detectors, imaging, spectroscopy

1 INTRODUCTION

Radiation detectors that combine good energy resolution with fine spatial resolution should find applications in many areas of research. Current challenges in high energy astrophysics require superior spectroscopy to resolve cyclotron features in highly magnetized neutron stars,[1] determine annihilation radiation line–width from the galactic plane,[2,3] and improve sensitivity to narrow-line features in a variety of astrophysical sources such as supernovae remnants.[4] Superior angular resolution is needed to localize unknown sources or to resolve closely spaced sources such as near the galactic center. Solar flare observations need good spectroscopy to observe the spectral change between soft, thermal and non-thermal emissions.

Applications for germanium strip detectors include coded-aperture imaging where good spectroscopy and high angular resolution are required. Compton scatter telescope imaging with sensitivity starting as low as 300 keV would improve on the success of COMPTEL on NASA's *Compton* Gamma Ray Observatory.[5] Imaging detectors are needed for the focal plane of a hard X-ray grazing-incidence

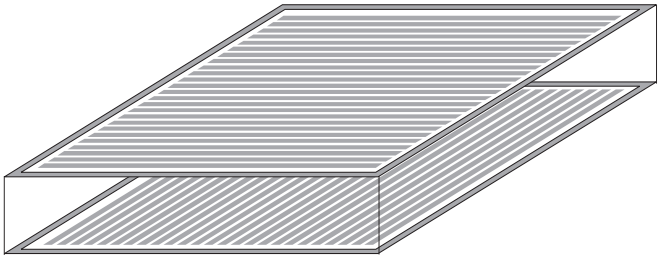

Figure 1: Schematic of the 2 mm pitch germanium strip detector. Crossed electrodes provide two-dimensional position localization of interactions. The electrodes are read out individually. The guard ring provides increased immunity to surface leakage currents. There are 25 strips on each face of the detector, centered on a 2 mm pitch and 50 mm long, providing 2 mm position resolution. The active volume is $50 \times 50 \times 10$ mm.

mirror that concentrates hard X-rays up to $\sim$100 keV. And finally, one-dimensional position sensitive detectors improve the performance of Fourier telescopes.[6] Fourier telescopes can provide arc-second angular resolution such as in the successful Japanese YOHKOH instrument imaging solar flares.[7]

In a two-dimensional detector, perpendicular strip electrodes are deposited on opposite faces of the device as shown in Figure 1. One contact is ohmic, the other is a blocking contact. A high voltage bias is applied to fully deplete the device. An interacting gamma ray produces a charge cloud of electrons and holes at the site of the interaction. Under the influence of the applied field, the charges drift to the strip electrodes on the opposite faces. The signal from each strip is a charge pulse which is measured using standard pulse-height analysis electronics on each electrode. Position of the interaction is determined by matching strips with equal signals on the opposite faces of the detector (the number of holes collected on one face of the detector is identical to the number of electrons collected on the other).

Reading out individual strips provides the best performance.[8] Each strip behaves as a single-channel germanium detector with energy resolution dominated by the usual factors of detector and feed-through capacitance, quality of the front-end electronics and electron-hole counting statistics. Alternative readout using a charge division network to reduce the number of channels of electronics has also been tested. Performance of capacitive[9,10] or resistive[11] charge division networks is degraded from the individual strip readout and does not allow multi-pixel interactions to be reconstructed. Because of the large number of readout channels and low power budget of a typical astrophysics application, we are developing custom CMOS electronics for readout of these detectors.[12] A prototype device has been fabricated, with 7 mW/channel power consumption (preamplifier through ADC), and with expected noise performance of better than 2.1 keV FWHM when connected to a typical strip detector.

2 PERFORMANCE

The 25×25 (Figure 1) and 5×5 strip detectors used in this work were fabricated using a photomask technique[13] to make the lithium drifted and boron implanted contacts. Our laboratory data acquisition system consists of 60 spectroscopy channels permitting all strips to be individually analyzed. The ADCs are read out through a CAMAC crate with a Macintosh computer. Histograms are displayed in real-time for diagnostics during data acquisition. Events are stored on disk in a compressed list-mode format for subsequent processing and image reconstruction.

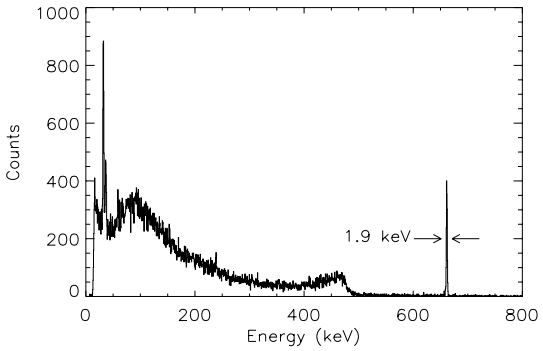

Figure 2: Energy spectrum of single pixel events from all 625 detector pixels. A ^{137}Cs source was used to uniformly illuminate the detector. The prominent features are the 662 keV γ-ray line, the barium K_α and K_β X-ray lines which are resolved from each other, and the Compton shelf.

2.1 Energy Resolution

The energy resolution of the strip detector is comparable to conventional germanium detectors. Interactions where the total energy is collected in a single strip provide the best energy resolution, primarily because only the noise from a single preamplifier affects the energy measurement. An energy spectrum made by selecting only the single pixel events is shown in Figure 2. Single pixels events are those with signals above threshold on only one boron and one lithium strip. Energy is measured using the signal on the boron electrodes. All of the boron strips are independently calibrated for gain and pedestal to within 0.1 keV at 662 keV. The histogram includes events from all 25 boron strips, with an over-all energy resolution of 1.9 keV FWHM at 662 keV. Photopeak interaction efficiency of $\sim$1% in a single strip is observed, which is consistent with the expectation that the majority of the interactions are photoelectric in a narrow strip.

The energy resolution of the 25×25 strip detector is shown in Table 1 for 60 and 662 keV γ-ray sources. Resolution is expressed as FWHM. The first column is resolution of a single strip with no other strips connected to the readout electronics. The second and third columns are single strip resolution with all 50 strips connected to our laboratory electronics. The slight loss in performance between columns 1 and 2 is attributed to ground loops, and a lower quality shaping amplifier that is normally used with the lithium strips.

Table 1
Energy resolution of single strip interactions

	E=60 (single strip)	E=60 (25 strips)	E=662
Boron	1.4	1.6	1.9
Lithium	1.9	2.6	3.0

A significant fraction of the γ-rays above $\sim$100 keV produce signals in more than one strip as shown in Figure 3. Events with multi-strip interactions are also usable. Boron-side events are straight-forward since crosstalk on this detector face is quite low ($\sim$0.1%). A spectrum of all events interacting in the detector, including those that produce signals in multiple strips is shown in Figure 4. The degraded energy resolution from 1.9 keV (Figure 2) is due to combining the noise from several preamplifiers for the majority of interactions.

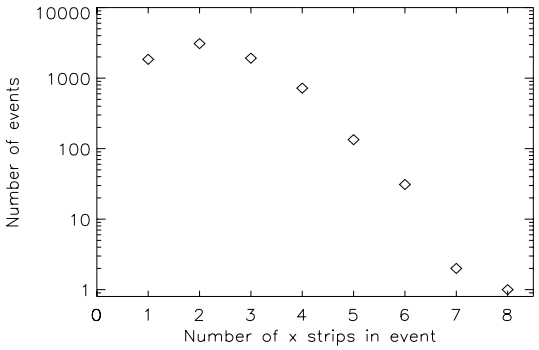

Figure 3: Distribution of the number of boron strips with signals above an energy threshold of 5 keV. A uniform illumination of 662 keV γ-rays is used, and events are selected that sum to the full energy absorption. Two strip interactions are the most probable, and multiple-strip interactions make up 70% of the total energy events.

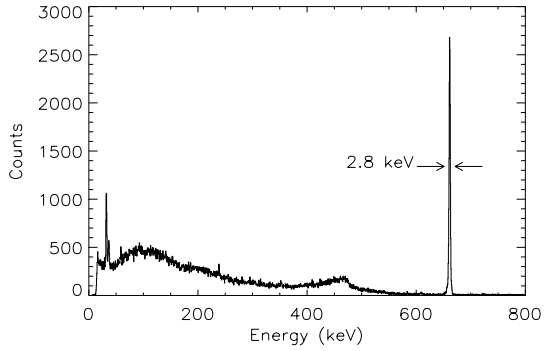

Figure 4: Energy spectrum from all events (both single and multi-strip interactions). A uniform illumination of 662 keV γ-rays was used. Photopeak efficiencies of $\sim$1% in a single strip, which is consistent with the Monte-Carlo predictions.

Crosstalk effects are more pronounced on the Li face of the detector because of the thickness of the Li strips ($\sim$300 μm for Li, *vs.* $\sim$1 μm for B). Measurements indicate typical crosstalk in our 25 $\times$ 25 detector is on the order of 1.5% between the lithium strips. Crosstalk between strips is measured using two-strip 662 keV photopeak events with signals S_i and S_j in adjacent strips. Each signal S_i produces a crosstalk signal $f_{ij}S_i$ in the adjacent strip. The crosstalk fraction f_{ij} is assumed to be symmetric, *i.e.* $f_{ij} = f_{ji}$. Thus the measured photopeak energy is:

$$E_{pp} = (1 + f_{ij})(S_i + S_j) > 662 \ \ \text{keV} \tag{1}$$

Calibration results for the lithium strips are shown in Figure 5. It is interesting to note that the first nine gaps between electrodes strips are wider than the remaining fifteen gaps. This was done intentionally in order to study the effects of the electrode gaps on the detector's performance. The wider gaps are 300 microns wider than the narrower gaps. The exact gap is not known because of lithium diffuses beyond the edge of the photo-mask during the electrode fabrication. We find that crosstalk is noticeably larger for the narrow gap strips, which implies that a significant portion of the crosstalk is from capacitance between the electrodes on the detector itself.

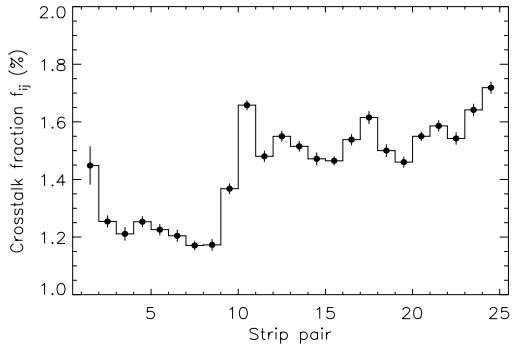

Figure 5: Crosstalk between lithium strips. Note that the gap between the first 10 Li strips is wider than for the rest resulting in a lower crosstalk.

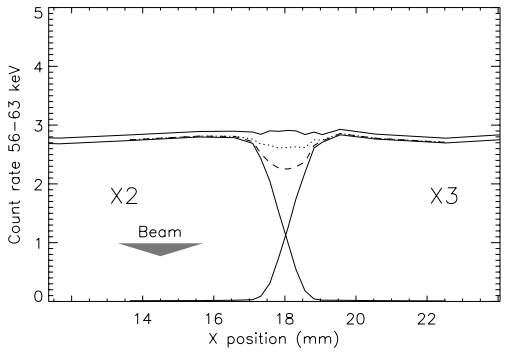

Figure 6: Response *vs.* position of a strip detector (9 mm strip pitch) to a 1.2 mm diameter (FWHM) collimated beam of 60 keV γ-rays. The beam is scanned across the boundary between two X-strips (B side). The γ-ray beam is incident on the Li strip face of the detector.

2.2 Position Resolution

The positional response of the 5×5 detector was investigated using a collimated source of 60 keV gamma rays from ^{241}Am. The strips on this detector are on a 9 mm pitch and 45 mm long. The active volume of the detector is 11 mm thick with an area of 45×45 mm. The collimated beam is $\sim$1.2 mm in diameter (FWHM) with a triangular intensity profile on the surface of the detector. The position of the beam is controlled by a position table under computer control.

Spatial response between two adjacent boron strips, X2 and X3, is shown in Figure 6. The source is moved along the length of one of the lithium strips. The count rate in the lithium strip is given by the upper solid curve and the lower solid curves are the count rates in the boron strips. There is a relatively flat response to 60 keV photopeak events over the surface of strip X2, then drops off rapidly to zero at the edge of the strip. Similarly, response of the X3 strip rises as X2 drops. A narrow region between strips is expected where charge is shared between adjacent strips. These charge sharing events between X2 and X3 are excluded from the individual strip response curves by event selection using a narrow energy window around 60 keV. Therefore, the sum of the individual strip responses (dashed curve) drops between the strips. The lithium strips have a similar sharp edge in response *vs.* position.

About half of the charge sharing events are recovered by summing the signals from adjacent strips. The dotted curve in Figure 6 represents the 60 keV window rate in the sum of the two strips. The remaining dip in the response curve is attributed to charge sharing events where the signal in one of the two strips is below our discriminator threshold ($\sim$20 keV), and is therefore not digitized.

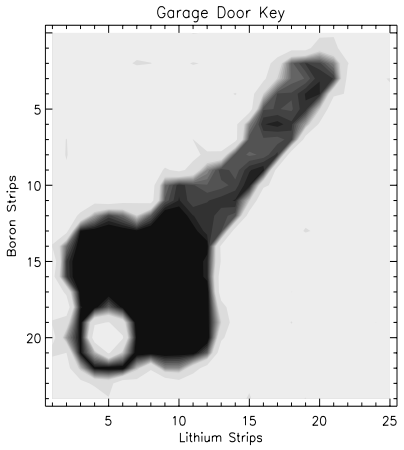

Figure 7: Shadowgram of a brass key using 60 keV γ-rays from ^{241}Am. The shaft of the key is thinner than the handle and therefore absorbs fewer γ-rays, appearing slightly lighter in this image.

The width of the charge-division region between strips can be estimated from the roll-off of the count rate at a strip edge. The fluence profile of the collimated beam is first calculated from the geometry of the collimator. The collimated beam has a triangular profile, as shown in Figure 6. The roll-off is then modeled as the response to this beam scanned over a strip edge. The true position of the strip edge is determined by moving an assumed position until the model fits the roll-off of the count rate. Results of fitting adjoining strip edges suggest a gap of $\sim$0.4 mm between both the X- and Y-strips where charge division occurs between the strips. This is consistent with the size of the gap between the electrodes. The sharpness of the roll-off compared with the beam profile suggest that the sharpness of the strip edge, *i.e.* the range of positions over which the count rate for full energy collection on a single strip drops from 90% to 10%, is less than 0.2 mm and possibly much finer.

3 IMAGING

In order to demonstrate the imaging capabilities of these detectors, we have produced a transmission image of a brass key. In the simplest imaging mode, only single site interactions are used. Figure 7 was produced by illuminating a garage door key with 60 keV γ-rays from ^{241}Am. The shadow of the key was projected on the detector's imaging surface. Noise in this image is primarily due to counting statistics, with an average of roughly 60 counts per detector pixel in the white areas. There is more transmission through the shaft of the key where groves have been cut, making the shaft somewhat thinner than the handle. The excellent energy resolution of the germanium detector can be used in the imaging mode. In the key-image, γ-rays were selected in the energy band from 56-62 keV. Energy resolution is a feature of these detectors, and can provide good rejection of scattered γ-rays which can add fog or increase background in an image. Scatter rejection is particularly effective at energies higher than 60 keV. Energy resolution may also be used with a broad spectrum source to probe an object with many energies simultaneously.

Germanium strip detectors are also good focal planes in a coded aperture imaging system. Besides astrophysics, an instrument like this may find applications in arms control[14] or radioactive waste imaging by providing good imaging with energy resolution. For a simple demonstration of near field imaging, a coded aperture was constructed from a tantalum sheet with 3 mm cell size (smallest opening). The

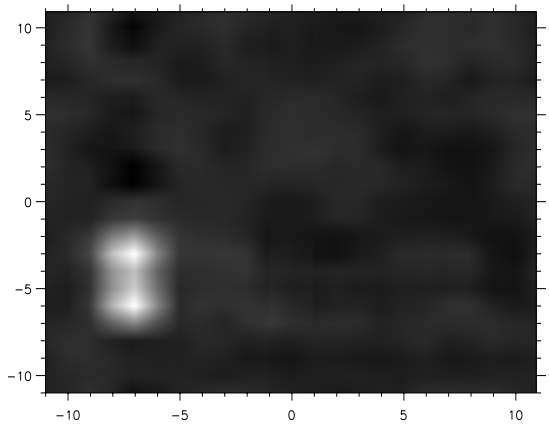

Figure 8: Coded aperture image of two closely spaced radioactive sources using the 25×25 strip detector. The coded aperture pattern is oversampled by the detector by a ratio of 2:1. The tick marks represent the size of detector pixels projected back into the imaging plane.

aperture was generated from an 11×11 fundamental pattern with 61 open cells. The telescope was designed to focus at 276 cm with a detector-aperture spacing of 92 cm. With this geometry, sources spaced by > 1.2 cm are fully resolved from each other in the reconstructed image. Figure 8 was produced by illuminating the coded-aperture telescope with ^{241}Am sources located about 2.0 cm apart from each other.

Germanium strip detectors can provide significant improvements in performance of Compton scatter telescopes. The principle of operation of these telescopes is to scatter a γ-ray in one detector (D1), then to absorb the scattered γ-ray in a second detector (D2). The scatter angle of the γ-ray in the first detector may be computed from the energy lost in the two detectors. The direction of the scattered γ-ray is determined from the position of the interactions in the two detectors. The direction of origin of each γ-ray is therefore localized to a cone about the direction of the scattered γ-ray with a cone half-angle equal to the scatter angle. The cone wall has a finite width governed by the uncertainties in energy and position measurements in the two detectors. Details about a Compton telescope concept called *ATHENA* using germanium strip detectors are presented elsewhere.[15,16]

A simple near-field Compton imager was constructed using the 25×25 as the D1 detector, and the 5×5 as the D2 detector. In astrophysical Compton telescopes, the two detector planes typically are parallel to each other. In our experiment the 25×25 detector is mounted vertically, while the 5×5 is horizontal due to detector constraints. The D1 detector was positioned 25 cm above and 40 cm in front of D2. An image of two point sources is shown in Figure 9. The dark point in Figure 9 shows the image of a ^{137}Cs source obtained with roughly 100 full energy events. The image was reconstructed on planes at various depths and the distance from the source to the detector (8 cm) was found by choosing the plane with the largest number of counts in a pixel or set of pixels. This method allows one to position the depth of a near-field object to $\sim$1 cm. The measured full width at half maximum of this source is 5 mm, whereas the actual source size was $\sim$3 mm. The lower set of ellipses in the figure shows another point source that is out of focus by 2.5 cm.

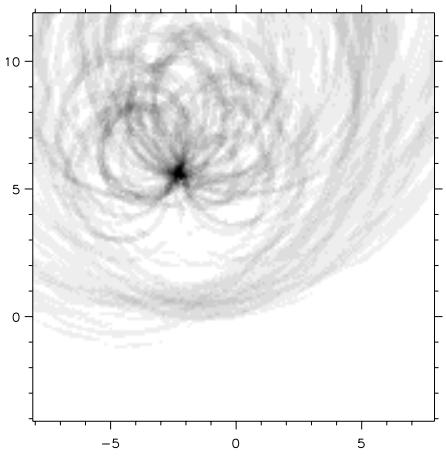

Figure 9: Compton telescope image made using two germanium strip detectors and two point sources. The image was reconstructed at a distance of 8 cm in front of the D1 detector. A second source was at a distance of 10.5 cm and about 60^o from the telescope axis. A total of $\sim$100 photons are detected from each point source.

4 CONCLUSIONS

We have demonstrated that the germanium strip detector can provide both good energy and spatial resolution, and that these properties are valuable in a number of applications. These detectors are ideal for imaging applications using transmission radiography, coded apertures, and Compton scatter techniques. We expect to have an array of four of the 2 mm pitch detectors by next year. This larger array will be used to further demonstrate imaging applications.

5 REFERENCES

1. Grove, J.E., *et al.*, 1995, ApJ 438, L25.
2. Johnson, W.N., et al., 1972, *Astrophys. J.*, **172**, L1.
3. Leventhal, M., et al., 1978, *Astrophys. J.*, **225**, L11.
4. Clayton, D.D., 1974, *Ap.J.*, **188**, 155.
5. Schoenfelder, V. et al., 1993, *ApJS*, **86**, 657.
6. Prince, T.A., *et al.* 1988, *Solar Physics*, **118**, 269.
7. Masuda, S., *et al.* 1994, *Nature*, **371**, 495.
8. Kroeger, R.A., *et al.* 1994, Proc. Imaging in High Energy Astronomy, Anacapri.
9. Inderhees, S.E., *et al.*, 1995, *Trans on Nucl Sci*, **42**, No. 4.
10. Kroeger, R.A., *et al.*, 1994, *Nucl Instr & Meth* A, **348**, 507.
11. Gerber, M.S. and Miller, D.W. 1976 *Nucl Instr. and Meth.*, **138**, 445.
12. Kroeger, R.A., *et al.*, 1995, *Trans on Nucl Sci*, **42**, No. 4.
13. Gutknecht D., *et al.* 1990, *Nuc. Instr. and Meth.*, **A228**, 1
14. Ziock, K.P., *et al.*, 1993, *IEEE Trans. Nucl. Sci.*, **39**, 4, 1046.
15. Johnson, W.N. *et al.* 1995, *Proc. Imaging in High Energy Astronomy*, Anacapri.
16. Johnson, W.N. *et al.* 1995, *This conference*